

A FORMULATION FOR WING AEROELASTIC ANALYSIS BASED ON THE UNSTEADY VLM AND STRUCTURAL DISCONTINUOUS GALERKIN TECHNIQUE

Fernando Montano¹, Ivano Benedetti¹ & Vincenzo Gulizzi¹

¹Department of Engineering, Università degli Studi di Palermo, Palermo, 90128, Italy

Abstract

This work proposes the conjoined use of the aerodynamic unsteady vortex lattice method (UVLM) and the structural discontinuous Garlerkin (DG) method for the general aeroelastic analysis of aircraft wings. While DG methods have been profitably employed for the analysis of solid and fluid mechanics, the coupling between DG methods and UVLM constitutes the novelty of the proposed study, which grants several advantages over more established approaches. The proposed DG structural formulation offers seamless higher order accuracy and straightforward coupling with the aerodynamic UVLM, which is implemented both in the planar and non-planar versions. In particular, different orders of accuracy can be easily selected in the structural model, both throughout the transverse section and along the span of the wing, thus offering the opportunity of tailoring the order of approximation to the features of the considered aeroelastic component. The obtained results agree well with available literature data and confirm the potential of the DG-UVLM framework for early aircraft conceptual analysis.

Keywords: Aeroelasticity, Flutter, Unsteady Vortex Lattice Method, Discontinuous Galerkin methods

1. Introduction

The capability of analysis the behaviour of structures operating in aerodynamic flows is of crucial importance for aeronautic and aerospace applications: poor aeroelastic design may have consequences ranging from simple performance degradation to catastrophic safety loss [1]. Aeroelastic analyses are becoming even more relevant due to the trend towards high aspect ratio, and thus more flexible, aircraft, motivated by the quest for higher aerodynamic efficiency, reduced fuel consumption, and more stringent environmental constraints.

Aeroelastic assessments must be considered in aircraft design since the very initial conceptual stage and often constitute the discriminating factor allowing the choice among different design options. In such initial stages of design, when several alternative architectures and structural configurations are generally considered, the availability of fast and reasonably accurate computational tools is an important industrial asset, while the employment of highly refined models, undoubtedly useful for detail and production design, might result unduly costly and time consuming. This motivates the interest in developing novel computational tools for effective and accurate preliminary aeroelastic analysis.

In the literature, different approaches have been developed for the analysis of aeroelastic problems, which include: high-fidelity frameworks coupling computational structural dynamics (CSD) and computational fluids dynamics (CFD) solvers [2, 3, 4, 5]; models adopting specific structural idealizations, aimed at reducing the cost of structural computations, coupled with CFD [6, 7, 8, 9, 10, 11, 12, 13]; reduced order modelling (ROM) strategies for reducing the cost of the aerodynamic analysis, while maintaining reasonable accuracy [14, 15, 16]; fast approaches based on beam or plate/shell structural models coupled with low/medium-fidelity aerodynamic models, such as the *vortex lattice method*

(VLM) that, although limited to specific flow regimes, offer acceptable estimates of the aerodynamic loads on lifting surfaces [17, 18, 19, 20].

The method developed here could be classified as belonging to the latter group. In this work, we propose a framework based on the combined use of a structural Interior Penalty discontinuous Galerkin (DG) method and an unsteady Vortex Lattice method (UVLM) for the analysis of dynamic aeroelastic problems. The work extends the approach successfully developed in Ref. [21], [22] for static aeroelastic analysis and it is built on a recent DG model for beams featuring general cross-sections, which allows using variable-order polynomial approximations for the structural analysis, enabling high-order accurate solutions for the wing problem [23].

The paper is organised as follows. Section 2.briefly introduces a schematic description of the analysed problem, providing the readers with some reference definitions. Section 3.discusses the DG formulation adopted for the wing structural analysis. The fundamentals of the unsteady VLM are briefly recalled in Section 4. while the coupling between the structural and aerodynamic models is detailed in Section 5. Eventually, the results of the computational tests are reported and discussed in Section 6. before drawing some *Conclusions* that confirm the potential of the developed framework for aeroelastic assessment in the conceptual stage of aircraft design.

2. Geometry description

Fig.(1) shows a schematic representation of the analysed aeroealastic system. Isotropic wings with generic transverse sections Ω and featuring taper, sweep and dihedral angles are considered. The geometry is described with respect to the body reference system $Ox_1x_2x_3$, defined according to standard aeronautics conventions, with the x_1 axis identified by the orthogonal projection of the wing root section chords over the aircraft symmetry plane. A gap $\Delta/2$ between the wing root sections and the aircraft symmetry plane is considered for generality, to account for the possible presence of the fuselage. The location $\mathbf{x} \equiv (x_1, x_2, x_3)^T$ of a generic point within the wing is identified by the mapping

$$\mathbf{x} = \mathbf{x}(\xi_1, \xi_2, \xi_3),$$
 (1)

where the coordinate ξ_2 spans the line $\mathscr L$ of the quarter-chord points of the wing, i.e. $\xi_2 \in \mathscr L \equiv [0,L]$, being L the length of $\mathscr L$, and the coordinates (ξ_1,ξ_3) span the wing cross-section, i.e. $(\xi_1,\xi_3) \in \Omega$. Eventually, the wing cross-section may be a bulk solid or consist of a thin-walled structure, as in the case sketched in Fig.(1a). Finally, the wing is subject to an incoming aerodynamic flow with velocity \mathbf{V}_{∞} forming an angle α with the x_1 axis.

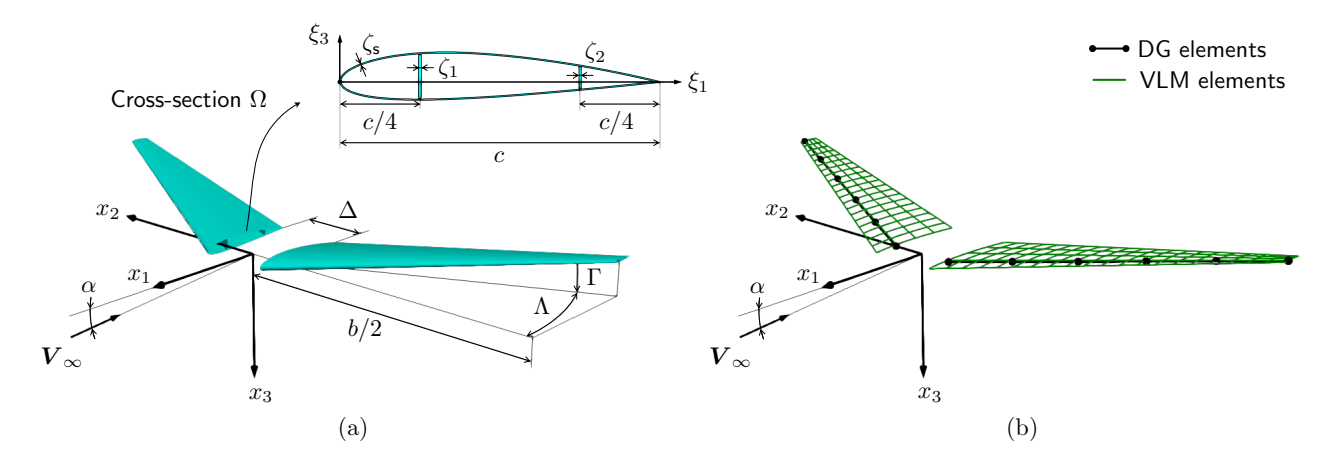


Figure 1 – (a) Wings structural arrangement: the wings feature generic cross-section Ω , lying on planes parallel to the reference plane x_1x_3 ; (b) Schematic representation of the 1D DG structural elements and of the aerodynamic VLM grid.

3. Structural model

3.1 Governing equations

The wing structure is assumed to undergo small deformations such that the strain-displacement relationship reads

$$\gamma = \mathbf{I}_k \frac{\partial \mathbf{u}}{\partial x_k},\tag{2}$$

where $\mathbf{u} \equiv (u_1, u_2, u_3)^{\mathsf{T}}$ denotes the displacement vector, $\gamma \equiv (\gamma_{11}, \gamma_{22}, \gamma_{33}, \gamma_{23}, \gamma_{13}, \gamma_{12})^{\mathsf{T}}$ denotes the vector containing the strain components in Voigt notation, and \mathbf{I}_k , with k = 1, 2, 3, are constant matrices containing ones and zeros only, whose explicit expression can be found in Refs.[23]. In Eq.(2) and in the continuation of the paper, the Einstein implicit summation notation is employed for repeated Latin subscripts taking values in $\{1, 2, 3\}$.

The material behavior is also assumed to be linear such that the relationship between strain and stress is expressed as

$$\sigma = \mathbf{C}\gamma,\tag{3}$$

where $\sigma \equiv (\sigma_{11}, \sigma_{22}, \sigma_{33}, \sigma_{23}, \sigma_{13}, \sigma_{12})^{\mathsf{T}}$ denotes the vector containing the stress components in Voigt notation and \mathbf{C} is the 6×6 matrix containing the stiffness coefficients.

Upon introducing the density ρ and the vector $\overline{\mathbf{b}} \equiv (\overline{b}_1, \overline{b}_2, \overline{b}_3)^{\mathsf{T}}$ of the external forces per unit volume, and following the hypotheses introduced above, the governing equations of the structural model read

$$\rho \frac{\partial^2 \mathbf{u}}{\partial t^2} - \frac{\partial}{\partial x_k} \left(\mathbf{C}_{kl} \frac{\partial \mathbf{u}}{\partial x_l} \right) = \overline{\mathbf{b}},\tag{4}$$

where $\mathbf{C}_{kl} \equiv \mathbf{I}_k^{\mathsf{T}} \mathbf{C} \mathbf{I}_l$.

3.2 Discontinuous Galerkin formulation

From the structural perspective, the wing is discretized into N_e non-overlapping elements along the line $\mathscr L$ of the quarter-chord points, such that the modeling domain $\mathscr D$ of the beam is approximated as $\mathscr D \approx \mathscr D^h \equiv \bigcup_{e=1}^{N_e} \mathscr D^e$, where $\mathscr D^e \equiv \Omega \times [y_-^e, y_+^e]$ is a generic e-th element, and y_-^e and y_+^e are the e-th element's end points along $\mathscr L$. This allows us to introduce the space $\mathscr V^{hp}$ of discontinuous basis functions as

$$\mathscr{V}^{hp} \equiv \{ v : \mathscr{D}^h \to \mathbb{R} \mid v(\xi \in \mathscr{D}^e) \in \mathscr{P}^p(\mathscr{D}^e) \ \forall e = 1, \dots, N_e \},$$
 (5)

where $\mathscr{P}^p(\mathscr{D}^e)$ is the space of tensor-product polynomials up to degree p defined over the element \mathscr{D}^e . It is then possible to show that the DG solution \mathbf{u}^h of Eq.(4) must satisfy

$$B_t(\mathbf{V}, \mathbf{u}^h) + B_{DG}(\mathbf{V}, \mathbf{u}^h) = L_{DG}(\mathbf{V}, \overline{\mathbf{b}})$$
(6)

for any $\mathbf{V} \in (\mathscr{V}^{hp})^3$, where

$$B_t(\mathbf{V}, \mathbf{u}^h) \equiv \int_{\mathcal{P}^h} \rho \mathbf{V}^{\mathsf{T}} \frac{\partial^2 \mathbf{u}^h}{\partial t^2} dV, \tag{7}$$

$$B_{\text{DG}}(\mathbf{V}, \mathbf{u}^h) \equiv \int_{\mathscr{D}^h} \frac{\partial \mathbf{V}^{\intercal}}{\partial x_k} \mathbf{C}_{kl} \frac{\partial \mathbf{u}^h}{\partial x_l} dV + \\ - \int_{\mathscr{D}^h} \left([\![\mathbf{V}]\!]_k^{\intercal} \left\{ \mathbf{C}_{kl} \frac{\partial \mathbf{u}^h}{\partial x_l} \right\} + \left\{ \frac{\partial \mathbf{V}^{\intercal}}{\partial x_k} \mathbf{C}_{kl} \right\} [\![\mathbf{u}^h]\!]_l \right) dS + \int_{\mathscr{D}^h} \mu [\![\mathbf{V}]\!]^{\intercal} [\![\mathbf{u}^h]\!] dS + \\ - \int_{\Omega(\xi_2 = 0)} \left(n_k \mathbf{V}^{\intercal} \mathbf{C}_{kl} \frac{\partial \mathbf{u}}{\partial x_l} + \frac{\partial \mathbf{V}^{\intercal}}{\partial x_k} \mathbf{C}_{kl} \mathbf{u}^h n_l \right) dS + \int_{\Omega(\xi_2 = 0)} \mu \mathbf{V}^{\intercal} \mathbf{u}^h dS \quad (8)$$

and

$$L_{\mathsf{DG}}(\mathbf{V}, \overline{\mathbf{b}}) \equiv \int_{\mathscr{D}^h} \mathbf{V}^{\mathsf{T}} \overline{\mathbf{b}} \, \mathrm{d}V. \tag{9}$$

In Eqs.(7), (8), and (9), the terms $\int_{\mathscr{D}^h} \bullet \, \mathrm{d}V \equiv \sum_e \int_{\mathscr{D}^e} \bullet \, \mathrm{d}V$ and $\int_{\mathscr{I}^h} \bullet \, \mathrm{d}S \equiv \sum_i \int_{\Omega(\xi_2 = y^i)} \bullet \, \mathrm{d}S$, denotes the so-called broken integrals, where y^i is the location of a generic i-th interface between two adjacent elements along the quarter-chord-point line \mathscr{L} . Eventually, n_k is the k-th component of the element's

outward unit normal, while the terms $\{\bullet\}$ and $[\![\bullet]\!]$ denotes the so-called average and jump operators, which are defined as

 $\{\bullet\} \equiv \frac{1}{2} (\bullet^e + \bullet^{e+1}) \quad \text{and} \quad [\![\bullet]\!]_k \equiv \bullet^e n_k^e + \bullet^{e+1} n_k^{e+1}.$ (10)

Finally, it is worth noting the weak form given in Eq.(6) is an extension to beam elasto-dynamics of a recently-developed class of Interior Penalty discontinuous Galerkin solvers for various structural components, such as beams [23], plates [24, 25] and shells [26, 27, 28, 29]. It is also worth noting that, upon integration over the wing cross-section, the present discretization consists of a set of one-dimensional DG structural elements that are attached to the quarter-chord-point line of the wing, as sketched in Fig.(1b).

3.3 Semi-discrete structural model

Upon evaluating the element integrals and following a standard assembly procedure, Eq.(6) leads to the following semi-discrete set of ordinary differential equations

$$\mathbf{M}_{\mathsf{S}}\ddot{\mathbf{X}} + \mathbf{K}_{\mathsf{S}}\mathbf{X} = \mathbf{F}_{\mathsf{S}} \tag{11}$$

where \mathbf{M}_S is the structural mass matrix, \mathbf{K}_S is the structural stiffness matrix, the vector \mathbf{X} collects the coefficients of the discontinuous basis functions and \mathbf{F}_S collects the components of the external forces. As discussed in the next section, the loading term \mathbf{F}_S depends on the aerodynamic flow and will provide the fluid-to-structure coupling. It is worth noting that Eq.(11) does not contain damping terms, which may be included using Rayleigh approach [30], whereby the structural damping matrix \mathbf{C}_S is defined as a linear combination of the mass and the stiffness matrices, i.e., $\mathbf{C}_S = \alpha_R \mathbf{M}_S + \beta_R \mathbf{K}_S$; here, α_R and β_R are suitably defined coefficients whose values are given during the discussion of the numerical results. Upon introducing such a damping term, Eq.(11) becomes

$$\mathbf{M}_{\mathsf{S}}\ddot{\mathbf{X}} + \mathbf{C}_{\mathsf{S}}\dot{\mathbf{X}} + \mathbf{K}_{\mathsf{S}}\mathbf{X} = \mathbf{F}_{\mathsf{S}}. \tag{12}$$

4. Aerodynamic model

The aerodynamic model is based on the UVLM [31], whereby the wing camber surface is replaced by a grid of aerodynamic panels and a ring vortex is attached to each panel; as such, the aerodynamic grid can be planar or non-planar, see e.g. [21] [22]. Figure (1b) shows a sample non-planar aerodynamic grid corresponding to the wing configuration shown in Fig.(1a).

When the lifting surfaces are modelled by N vortices, the aerodynamic impenetrability condition leads to a discrete system of equations of the form

$$\mathbf{A}(\mathbf{X})\Gamma = \mathbf{b}(\mathbf{X}, \dot{\mathbf{X}}, t). \tag{13}$$

In Eq.(13), $\bf A$ is a $N \times N$ matrix, Γ is the N-dimensional vector of unknown values of the ring vortices circulation, and $\bf b$ is the N-dimensional right-hand side, which contains terms stemming from the free-stream velocity, the motion of the structure, and the velocity induced by the wake vortices that are shed by the wing trailing edge.

The solution of the system given in Eq.(13) allows computing the forces acting on the wing structure. In particular, the force \mathbf{f}^p acting on a generic p-th panel is evaluated as follows, see, e.g., [32, 33],

$$\mathbf{f}^{p} = \rho_{\infty} \mathbf{v}^{p} \times \mathbf{l}^{p} \widetilde{\Gamma}^{p} + \rho_{\infty} \dot{\Gamma}^{p} A^{p} \mathbf{n}^{p}, \tag{14}$$

where ρ_{∞} is the density of the fluid, \mathbf{l}^p is the vector associated with leading segment of the attached ring vortex, \mathbf{v}^p is the local flow velocity evaluated at the midpoint of \mathbf{l}^p , and \mathbf{n}^p and A^p are the unit normal vector and the area, respectively, of the p-th panel. Additionally, $\dot{\Gamma}^p$ is the time-derivative of the attached vortex' circulation and $\tilde{\Gamma}^p$ is the circulation at the leading segment of the ring vortex; $\tilde{\Gamma}^p$ coincides with the circulation Γ^p of the attached vortex if the p-th panel is at the leading edge of the wing, or otherwise with the difference between the circulation values of two adjacent ring vortices along the chord direction.

5. Fluid-structure coupling

The aeroelastic problem is inherently coupled. In general, both aerodynamic loads ${\bf F}_A$ and non-aerodynamic loads ${\bf F}_S$, e.g. weight, act on the wing. Recalling Eqs.(12,13), the general aeroelastic system may be written as

$$\begin{cases} \mathbf{A}(\mathbf{X})\Gamma = \mathbf{b}(\mathbf{X}, \dot{\mathbf{X}}, t) \\ \mathbf{M}_{\mathsf{S}} \ddot{\mathbf{X}} + \mathbf{C}_{\mathsf{S}} \dot{\mathbf{X}} + \mathbf{K}_{\mathsf{S}} \mathbf{X} = \mathbf{F}_{\mathsf{S}}(t) + \mathbf{F}_{\mathsf{A}}(\Gamma, \dot{\Gamma}, t), \end{cases}$$
(15)

where the fluid-structure coupling is reflected both in the dependency of the VLM coefficients and right-hand side on X and \dot{X} and in the dependency of the aerodynamic forces on Γ , $\dot{\Gamma}$. The explicit dependency on time is expressed to allow for the consideration of independent external factors, e.g. the variation of the velocity of the incoming flow or general servo-mechanic actions on the lifting surface.

System (15) can be tackled adopting different schemes for different purposes or at different levels of approximation, as discussed also in Ref.[21] [22] for static aeroelastic problems. The linearized version of system (15) with respect to the equilibrium condition reads

$$\begin{cases} \mathbf{A}_{0}\Gamma = \mathbf{b}_{w} + \mathbf{b}_{1}\mathbf{X} + \mathbf{b}_{2}\dot{\mathbf{X}} \\ \mathbf{M}_{S}\ddot{\mathbf{X}} + \mathbf{C}_{S}\dot{\mathbf{X}} + \mathbf{K}_{S}\mathbf{X} = \mathbf{F}_{A1}\Gamma + \mathbf{F}_{A2}\dot{\Gamma} \end{cases}$$
(16)

where, the explicit dependece on t has been dropped, $\mathbf{A}_0 \equiv \mathbf{A}(\mathbf{X} = \mathbf{0})$, and

$$\mathbf{b}_{1} = \frac{\partial \mathbf{b}}{\partial \mathbf{X}}\Big|_{(\mathbf{X}, \dot{\mathbf{X}}) = \mathbf{0}} \quad \mathbf{b}_{2} = \frac{\partial \mathbf{b}}{\partial \dot{\mathbf{X}}}\Big|_{(\mathbf{X}, \dot{\mathbf{X}}) = \mathbf{0}} \quad \mathbf{F}_{A1} = \frac{\partial \mathbf{F}_{A}}{\partial \Gamma}\Big|_{(\Gamma, \dot{\Gamma}) = \mathbf{0}} \quad \mathbf{F}_{A2} = \frac{\partial \mathbf{F}_{A}}{\partial \dot{\Gamma}}\Big|_{(\Gamma, \dot{\Gamma}) = \mathbf{0}}, \tag{17}$$

is generally used for flutter analysis; eventually, in Eq.(16), \mathbf{b}_{w} represents the contribution of the wake to the induced velocity.

As customary for aeroelastic analysis, Eqs.(16) are formulated expressing the unknown vectors as $\mathbf{X} = \widetilde{\mathbf{X}} e^{pt}$ and $\Gamma = \widetilde{\Gamma} e^{pt}$, with $p = \sigma + j\omega \in \mathbb{C}$ being the generic complex eigenvalue, which leads to the classical flutter equations

$$[p^2\mathbf{M}_S + p\mathbf{C}_S + (\mathbf{K}_S - \mathbf{Q}(p))]\mathbf{X} = \mathbf{0},$$
(18)

where O is the generalized aerodynamic force matrix defined as

$$\mathbf{Q}(p) = (\mathbf{F}_{A1} + p\mathbf{F}_{A2})(\mathbf{A}_0 + \mathbf{A}_w(p))^{-1}(\mathbf{b}_1 + p\mathbf{b}_2), \tag{19}$$

with the term $\mathbf{A}_w(p)$ representing the effect of the wake on the wing's circulation. Eq.(18) is solved iteratively, adopting the standard p-k method, where $\mathbf{Q}(p)$ is replaced by $\mathbf{Q}(j\omega)$.

6. Computational results

The conjoined use of VLM and the structural DG method has already been successfully demonstrated for the static aeroelastic analysis of wings featuring arbitrary cross section in Ref.[22], where the method has been validated against literature data. As an example of the obtained results, Fig.(2) shows the wing-tip twist as a function of the free-stream velocity V_{∞} approaching the divergence speed V_D for a wing with rectangular plan-form and aspect ratio equal to 5. For further discussion the reader is referred to Ref.[22].

The framework has thus been extended to include the presence of structural dynamics and unsteady aerodynamics, so to enable the analysis of transient aerodynamic problems and aeroelastic flutter.

Fig.(3) shows few snapshots of the evolution of the wake shed by a rectangular wing, as obtained from the implemented in-house UVLM code, which is being coupled with the dynamic DG structural method.

Fig.(4) shows the results of the free-vibration analysis of a wing with rectangular planform and sweep angle Λ , as that analysed in Ref.[34], to which the readers are referred for further details. The figure compares the frequencies computed for the first four structural modes using a DG₅ scheme with those obtained in Ref.[34] using a FE plate theory.

Fig.(5) reports the results of the flutter analysis of the same wing considered above, with the sweep angle set to $\Lambda=20^{\circ}$. The analysis has been performed implementing the p-k method within the DG-UVLM framework. The results are compared with those obtained using the aeroelastic module of NASTRAN, which agree well with those reported in Ref.[34].

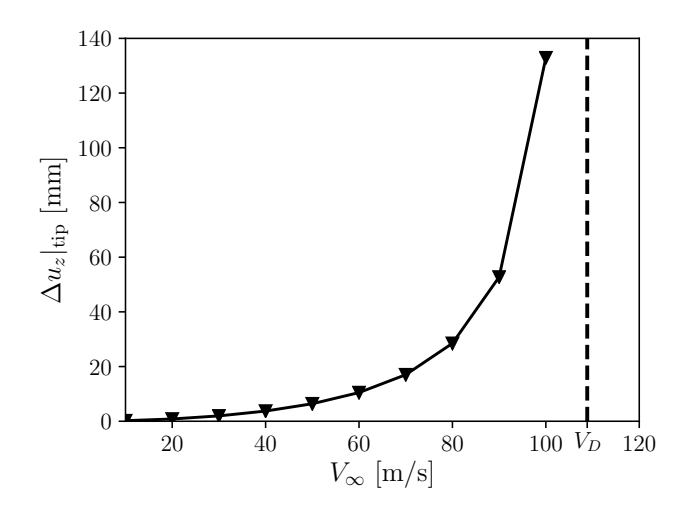


Figure 2 – Effect of the free-stream velocity on the wing tip twist for the wing configuration analysed in Ref.[22]. The plot shows how the method is able to capture the wing static divergence.

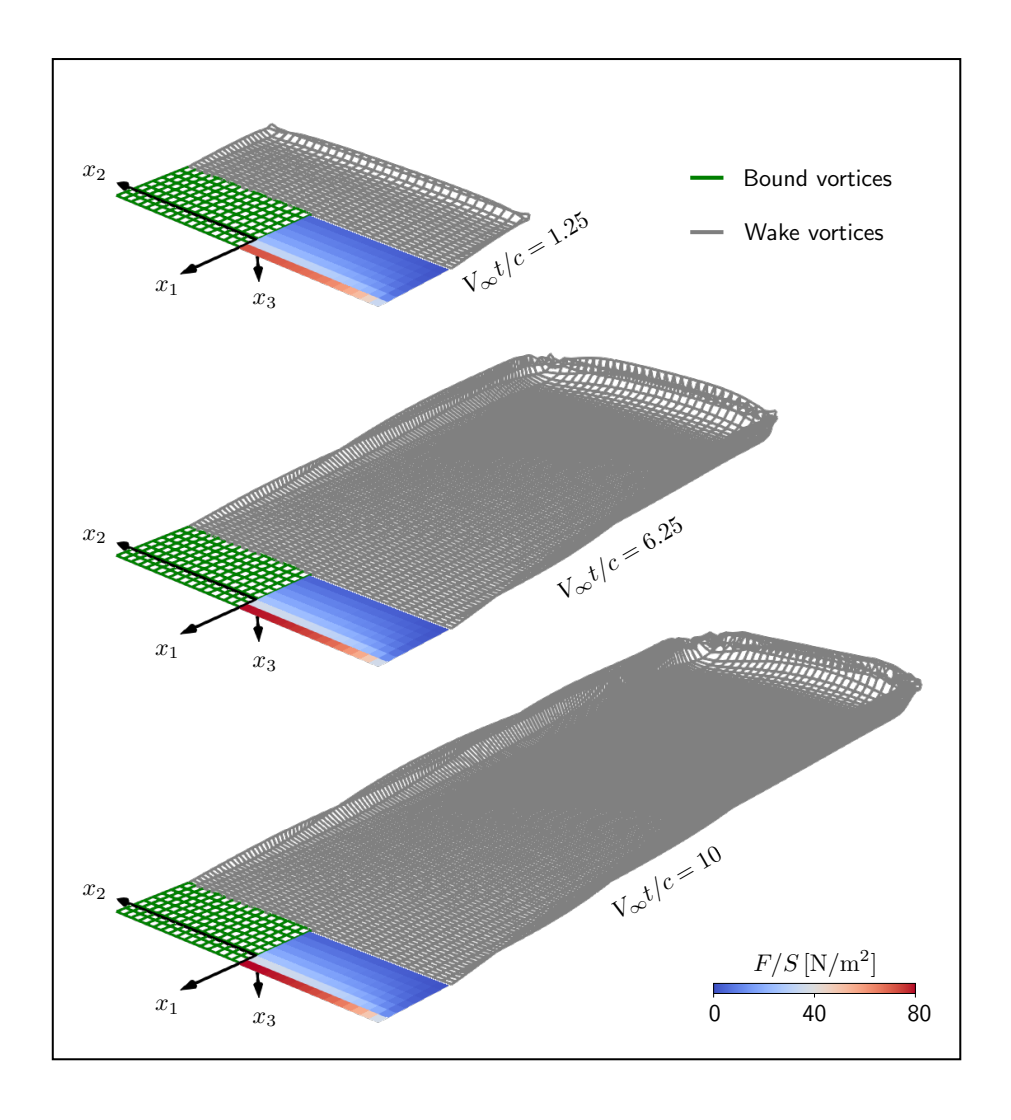


Figure 3 – Wake evolution and force distribution for a rectangular wing with aspect ratio equal to 4 as reconstructed by the implemented UVLM to be coupled with the DG structural method.

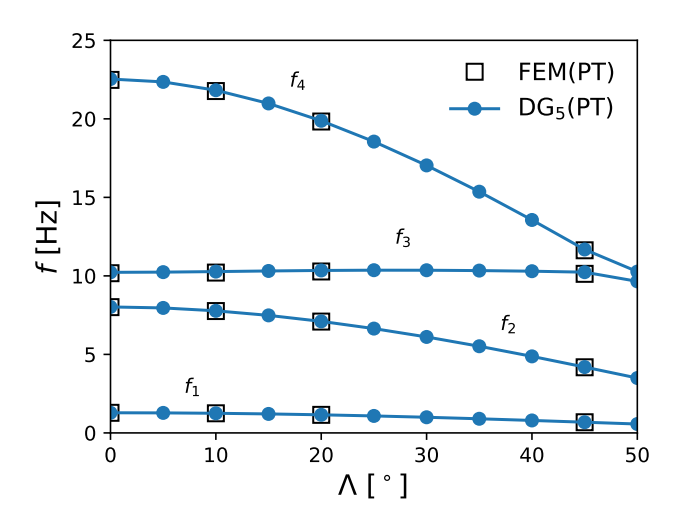


Figure 4 – Predicted values of frequency versus sweep angle for the first four structural modes of the wing considered in Ref.[34].

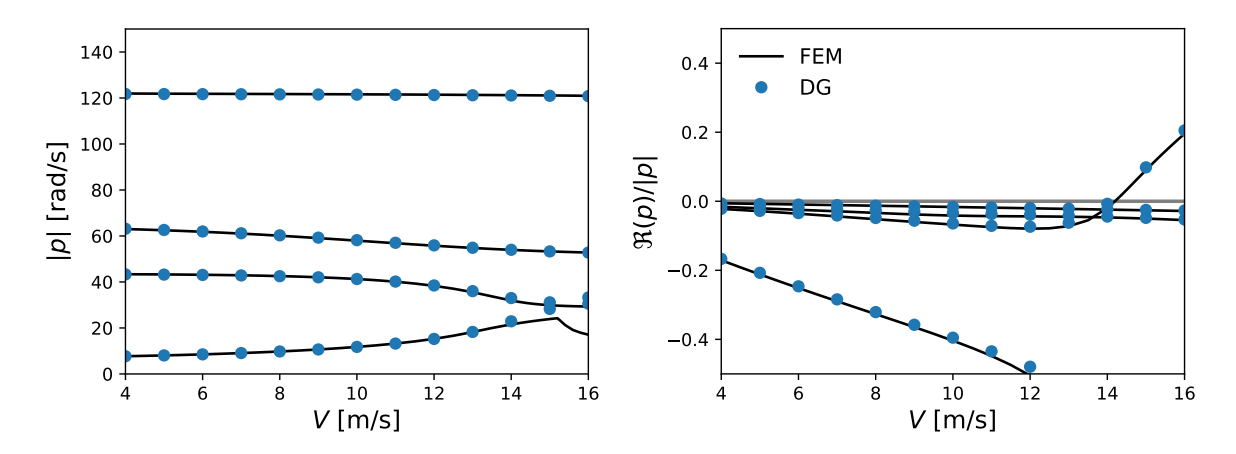


Figure 5 – Flutter analysis of a rectangular wing with sweep $\Lambda=20^{\circ}$ – see Ref.[34] for details. The analysis has been performed implementing the p-k method in the proposed DG-UVLM computational framework.

7. Conclusions

In this contribution a novel framework for dynamic aeroelastic analysis has been formulated, developed, implemented and validated. The scheme is based on the simultaneous use of a discontinuous Galerkin method for the structural analysis of beams or shells and of an unsteady VLM for the representation of the unsteady aerodynamics. The method had already been proven apt to capture static aeroelastic responses, while in this work it has been validated for dynamic aeroelasticity by a standard p-k method. The flexibility of the structural model, which may represent generalized kinematics, and the ease of coupling with the UVLM make the method suitable for early aeroelastic assessment in conceptual aircraft design, which will be explored in future investigations.

8. Contact Author Email Address

mailto: vincenzo.gulizzi@unipa.it

9. Acknowledgments

FM and IB acknowledge the support of the European Union and the Italian Ministry of University and Research through the PON 2014-2020, Asse IV - Istruzione e ricerca per il recupero - REACT-EU, Azioni IV.4 e IV.6 - Contratti di ricerca su tematiche green e sui temi dell'innovazione, FSE and REACT-EU funds , DM 1062/2021. FM and VG acknowledge the support of the Department of Engineering of the University of Palermo, Italy through the grant *Gruppi di ricerca 2022*.

10. Copyright Statement

The authors confirm that they, and/or their company or organization, hold copyright on all of the original material included in this paper. The authors also confirm that they have obtained permission, from the copyright holder of any third party material included in this paper, to publish it as part of their paper. The authors confirm that they give permission, or have obtained permission from the copyright holder of this paper, for the publication and distribution of this paper as part of the ICAS proceedings or as individual off-prints from the proceedings.

References

- [1] Allan Larsen. Aerodynamics of the tacoma narrows bridge 60 years later. *Structural Engineering International*, 10(4):243–248, 2000.
- [2] Jianming Hao and Teng Wu. Downburst-induced transient response of a long-span bridge: A cfd-csd-based hybrid approach. *Journal of Wind Engineering and Industrial Aerodynamics*, 179:273–286, 2018.
- [3] Marcel Ilie. A fully-coupled cfd/csd computational approach for aeroelastic studies of helicopter blade-vortex interaction. *Applied Mathematics and Computation*, 347:122–142, 2019.
- [4] Dong Ok Yu and Oh Joon Kwon. Predicting wind turbine blade loads and aeroelastic response using a coupled cfd–csd method. *Renewable Energy*, 70:184–196, 2014. Special issue on aerodynamics of offshore wind energy systems and wakes.
- [5] Haris Hameed Mian, Gang Wang, and Zheng-Yin Ye. Numerical investigation of structural geometric non-linearity effect in high-aspect-ratio wing using cfd/csd coupled approach. *Journal of Fluids and Structures*, 49:186–201, 2014.
- [6] M Smith, M Patil, and D Hodges. Cfd-based analysis of nonlinear aeroelastic behavior of high-aspect ratio wings. In 19th AIAA applied aerodynamics conference, page 1582, 2001.
- [7] G. P. Guruswamy. Computational-fluid-dynamics- and computational-structural-dynamics-based time-accurate aeroelasticity of helicopter rotor blades. *Journal of Aircraft*, 47(3):858–863, 2010.
- [8] Luciano Demasi, Yonas Ashenafi, Rauno Cavallaro, and Enrico Santarpia. Generalized unified formulation shell element for functionally graded variable-stiffness composite laminates and aeroelastic applications. *Composite Structures*, 131:501–515, 2015.
- [9] Lin Wang, Xiongwei Liu, and Athanasios Kolios. State of the art in the aeroelasticity of wind turbine blades: Aeroelastic modelling. *Renewable and Sustainable Energy Reviews*, 64:195–210, 2016.
- [10] M. Sayed, Th. Lutz, E. Krämer, Sh. Shayegan, A. Ghantasala, R. Wüchner, and K.-U. Bletzinger. High fidelity cfd-csd aeroelastic analysis of slender bladed horizontal-axis wind turbine. *Journal of Physics: Conference Series*, 753(4):042009, sep 2016.
- [11] M Sayed, P Bucher, G Guma, T Lutz, and R Wüchner. Aeroelastic simulations based on high-fidelity cfd and csd models. *Handbook of Wind Energy Aerodynamics*, pages 1–76, 2022.

- [12] Marco Grifò, Andrea Da Ronch, and Ivano Benedetti. A computational aeroelastic framework based on high-order structural models and high-fidelity aerodynamics. *Aerospace Science and Technology*, 132:108069, 2023.
- [13] Marco Grifò, Vincenzo Gulizzi, Alberto Milazzo, Andrea Da Ronch, and Ivano Benedetti. High-fidelity aeroelastic transonic analysis using higher-order structural models. *Composite Structures*, 321:117315, 2023.
- [14] Sorin Munteanu, John Rajadas, Changho Nam, and Aditi Chattopadhyay. Reduced-order-model approach for aeroelastic analysis involving aerodynamic and structural nonlinearities. *AIAA Journal*, 43(3):560–571, 2005.
- [15] Jiaqing Kou and Weiwei Zhang. A hybrid reduced-order framework for complex aeroelastic simulations. *Aerospace Science and Technology*, 84:880–894, 2019.
- [16] Dongfeng Li, Andrea Da Ronch, Gang Chen, and Yueming Li. Aeroelastic global structural optimization using an efficient cfd-based reduced order model. *Aerospace Science and Technology*, 94:105354, 2019.
- [17] Joseba Murua, Rafael Palacios, and J. Michael R. Graham. Applications of the unsteady vortex-lattice method in aircraft aeroelasticity and flight dynamics. *Progress in Aerospace Sciences*, 55:46–72, 2012.
- [18] Erasmo Carrera, Alberto Varello, and Luciano Demasi. A refined structural model for static aeroelastic response and divergence of metallic and composite wings. *CEAS Aeronautical Journal*, 4(2):175–189, 2013.
- [19] M. Petrolo. Flutter analysis of composite lifting surfaces by the 1d carrera unified formulation and the doublet lattice method. *Composite Structures*, 95:539–546, 2013.
- [20] Changchuan Xie, Libo Wang, Chao Yang, and Yi Liu. Static aeroelastic analysis of very flexible wings based on non-planar vortex lattice method. *Chinese Journal of Aeronautics*, 26(3):514–521, 2013.
- [21] F. Montano, I. Benedetti, and V. Gullizzi. Stability and flying qualities analysis of flexible aircraft by coupling the Vortex Lattice Method and the discontinuous Galerkin method. In Aerospace Europe Conference 2023, 10th EUCASS, 9th CEAS, 2023.
- [22] Vincenzo Gulizzi and Ivano Benedetti. Computational aeroelastic analysis of wings based on the structural discontinuous galerkin and aerodynamic vortex lattice methods. Aerospace Science and Technology, 144:108808, 2024.
- [23] Vincenzo Gulizzi, Ivano Benedetti, and Alberto Milazzo. High-order accurate beam models based on discontinuous Galerkin methods. *Aerotecnica Missili & Spazio*, pages 1–16, 2023.
- [24] V. Gulizzi, I. Benedetti, and A. Milazzo. An implicit mesh discontinuous Galerkin formulation for higher-order plate theories. *Mechanics of Advanced Materials and Structures*, 27(17):1494–1508, 2020.
- [25] V. Gulizzi, I. Benedetti, and A. Milazzo. A high-resolution layer-wise discontinuous Galerkin formulation for multilayered composite plates. *Composite Structures*, 242:112137, 2020.
- [26] G. Guarino, A. Milazzo, and V. Gulizzi. Equivalent-single-layer discontinuous Galerkin methods for static analysis of multilayered shells. *Applied Mathematical Modelling*, 98:701–721, 2021.
- [27] G. Guarino, V. Gulizzi, and A. Milazzo. High-fidelity analysis of multilayered shells with cut-outs via the discontinuous Galerkin method. *Composite Structures*, 276:114499, 2021.
- [28] G. Guarino, V. Gulizzi, and A. Milazzo. Accurate multilayered shell buckling analysis via the implicit-mesh discontinuous Galerkin method. *AIAA Journal*, 60(12):6854–6868, 2022.
- [29] G Guarino, V Gulizzi, and A Milazzo. Transient and free-vibration analysis of laminated shells through the discontinuous galerkin method. In *ICAS Proceedings of the 33th Congress of the International Council of the Aeronautical Sciences*, Sweden, 2022.
- [30] Man Liu and D.G. Gorman. Formulation of rayleigh damping and its extensions. *Computers & Structures*, 57(2):277–285, 1995.
- [31] Joseph Katz and Allen Plotkin. *Low-Speed Aerodynamics*. Cambridge Aerospace Series. Cambridge University Press, 2 edition, 2001.
- [32] Robert JS Simpson, Rafael Palacios, and Joseba Murua. Induced-drag calculations in the unsteady vortex lattice method. *AIAA journal*, 51(7):1775–1779, 2013.
- [33] Thomas Lambert and Grigorios Dimitriadis. Induced drag calculations with the unsteady vortex lattice method for cambered wings. *AIAA Journal*, 55(2):668–672, 2017.
- [34] G. Dimitriadis, N.F. Giannelis, and G.A. Vio. A modal frequency-domain generalised force matrix for the unsteady vortex lattice method. *Journal of Fluids and Structures*, 76:216–228, 2018.